

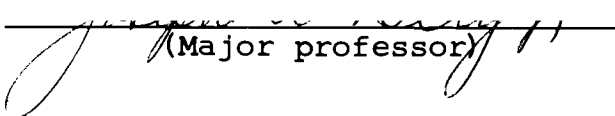
AN ABSTRACT OF THE THESIS OF

James Hall Whitcomb for the Master of Science in Oceanography
(Name) (Degree) (Major)

Date thesis is presented August 27, 1964

Title MARINE GEOPHYSICAL STUDIES OFFSHORE--
NEWPORT, OREGON

Redacted for Privacy

Abstract approved 
(Major professor)

A marine geophysical study using shallow seismic reflection, gravity and magnetic methods of investigation was done for an offshore area near Newport, Oregon. The area is bounded by the latitudes $44^{\circ}10'$ to $44^{\circ}50'$ N. and longitudes $124^{\circ}07'$ to $124^{\circ}30'$ W.

The interpretation of observational data showed that the geology of the area north of latitude $44^{\circ}25'$ N. consists of a north-south syncline. A geological, two-dimensional model was constructed to agree with the observed gravity and geological data along an east-west cross section in the area. The model's synclinal axis was found to shift to the west with depth. Basement depths of 19,000 to 21,500 feet were given in the deepest portion of the model syncline. If regional gravity decreases to the west, the model would have to be made shallower, and the axis

shift to the west would be less pronounced.

Seismic data indicate complex minor folding and possible faulting in the central portion of the area of investigation (central and southern Stonewall Bank). Gravity and magnetic readings indicate a rise of the basement in the western part of the area (west of Stonewall Bank).

The geology of the area south of latitude $44^{\circ}25'$ N. was interpreted to be a large, crystalline rock mass with its upper surface at shallow depths off Cape Perpetua. Gravity and magnetic data indicate that the crystalline mass noses down to the northwest. Geological models, that were constructed in this area to agree with gravity and geological data, indicate that the mass is probably cone-shaped, and the basement of the surrounding country rock is 13,000 to 16,000 feet deep. Shallow volcanic flows may be present in this area.

MARINE GEOPHYSICAL STUDIES OFFSHORE--NEWPORT, OREGON

by

JAMES HALL WHITCOMB

A THESIS

submitted to

OREGON STATE UNIVERSITY

in partial fulfillment of
the requirements for the
degree of

MASTER OF SCIENCE

June 1965

APPROVED:

Redacted for Privacy

Professor of Oceanography
In Charge of Major

Redacted for Privacy

Chairman of Department Oceanography

Redacted for Privacy

Dean of Graduate School

Date thesis is presented August 27, 1964

Typed by Sandra McMurdo

ACKNOWLEDGMENTS

This research was conducted under the direction of Professor Joseph W. Berg, Jr., Department of Oceanography, Oregon State University. The author extends his appreciation to Dr. Berg for his guidance and advice throughout the work. Appreciation is expressed to Dr. Peter Dehlinger for providing information concerning the reliability of the surface ship gravity data and terrain corrections. Discussions with Dr. John Byrne about the geology of the area were very helpful.

Mr. Wilber Rinehart programmed the two-dimensional gravity formula for the IBM 1620 computer. Dr. Parke Snavely of the U. S. Geological Survey provided density measurements for the geologic column along the coast near the area of interest. Mr. Neal Maloney gave helpful information about marine rock samples in the area. Mr. William Bales rebuilt part of the electrical system of the sparker and gave helpful suggestions about the instrumentation after it was operational.

This research was sponsored by the Office of Naval Research under contract Nonr 1286(02), Project 083-102. The National Science Foundation sponsored the magnetic measurement program under Grant GP2186.

TABLE OF CONTENTS

I.	INTRODUCTION.....	1
II.	BATHYMETRY.....	4
III.	SEISMIC REFLECTIONS.....	7
	Instrumentation.....	7
	Operation Technique.....	11
	Interpretation.....	12
	Seismic Reflection Results.....	15
IV.	GRAVITY.....	19
	Free-air Anomaly Map.....	19
	Cross Section A-A'.....	26
	Bouguer Anomaly.....	26
	Two-dimensional Model Development.....	27
	Results.....	32
	Cross Section B-B'.....	34
	Bouguer Anomaly.....	34
	Two-dimensional Model Development.....	35
	Results.....	37
V.	MAGNETICS.....	39
	Section Along C-C'.....	41
	Section Along D-D'.....	45
VI.	SUMMARY AND CONCLUSIONS.....	47
VII.	BIBLIOGRAPHY.....	50

FIGURES

1.	Index map showing the survey area in relation to the Oregon coast.....	2
2.	Bathymetric chart of the survey area.....	5
3.	Seismic composite map of the survey area.....	8
4.	Free-air gravity anomaly chart of the survey area..	21
5.	Bottom topography, terrain correction, and gravity of line A-A' (see Fig. 4).....	23
6.	Free-air gravity anomaly extending from shore line to 70 nautical miles along latitude 44°35' N. (This profile is along interpretative line A-A'.)..	25
7.	Geology, interpretative geological model and gravity along line A-A' (see Fig. 4).....	28
8.	Observed and calculated Bouguer gravity anomalies and interpretative geological models along line B-B' (see Fig. 4).....	36
9.	Total magnetic intensity map of the survey area....	40
10.	Magnetic sections along C-C' and D-D' (see Fig. 9).	42

TABLES

I. DEPTH VS. VELOCITY..... 13

II. MAGNETIC READING COMPARISONS AT TRACK INTER-
SECTIONS..... 39

MARINE GEOPHYSICAL STUDIES OFFSHORE--NEWPORT, OREGON

INTRODUCTION

The purpose of this research was to combine geophysical data from shallow seismic reflection, gravity, and magnetic surveys to determine, as nearly as possible, sub-bottom geological structural conditions off Newport, Oregon. In doing so, it may be possible to determine to what extent the geology along the coast can be extended beneath the sea. Initially, the area was chosen because underwater gravity measurements comprising a marine gravity range were available in it. Fig. 1 is an index map showing the survey area bounded by the coordinates 44°10' to 44°50' N. latitudes and 124°07' to 124°30' W. longitudes. The survey extended from Depoe Bay in the north to Heceta Head in the south.

The geophysical data were obtained by the Geophysics Research Group of Oregon State University beginning with extensive underwater gravity measurements which established the Marine Gravity Range, Newport, Oregon (12, p. 1-11) in the summer of 1962. A continuous seismic profiler was used over the same area in the summer of 1963 to obtain reflections from shallow (50 to 500 feet below bottom) geologic horizons. Magnetic measurements in the survey area were taken during 1963 and 1964.

In this paper the investigation is developed in the following order: topography, seismic reflections, gravity,

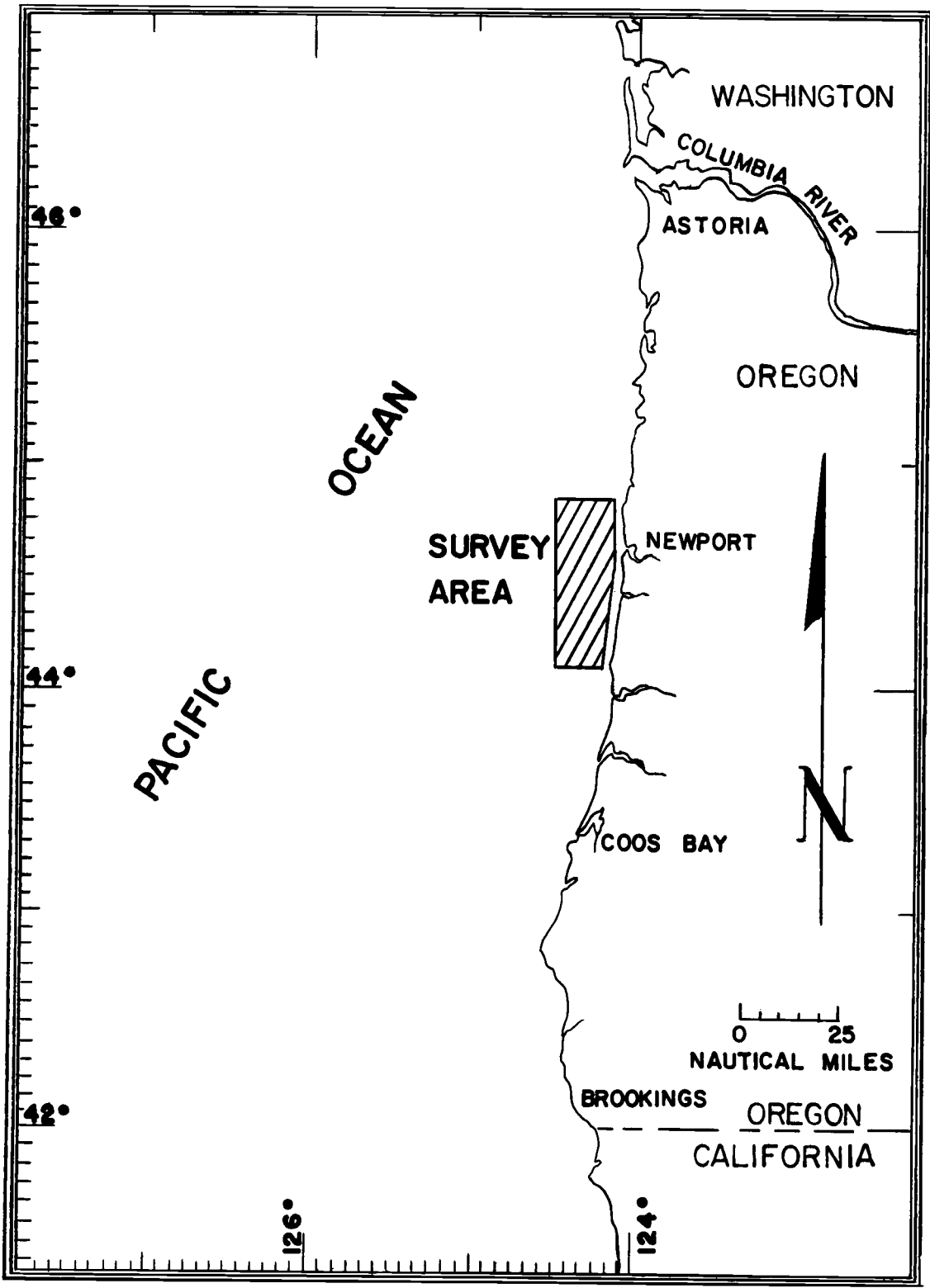


Figure 1. Index map showing the survey area in relation to the Oregon coast

and magnetics. In all of these topics, with the exception of seismic reflections, the data and their discussion are presented first, followed by a section of interpretation. The interpretation includes cross sections which illustrate the principal structure of the survey area as deduced from the geophysical data. Because the seismic reflection data were gathered and reduced by the author, the section in which they are presented begins with a description of instrumentation and interpretation. Finally, a summary of the results attempts to tie all of the methods into one structural interpretation of the survey area.

BATHYMETRY

Byrne (2, p. 65-74) contoured ocean bottom bathymetry using data collected from unpublished soundings of the U. S. Coast and Geodetic Survey and Precision Depth Recordings obtained by the Department of Oceanography, Oregon State University. Areal density of soundings on the continental shelf averages from 15 to 20 per square mile on the continental shelf to only 2 to 5 soundings per square mile on the continental slope. To correspond to the sounding densities, a chart contour interval of 10 fathoms was used to a depth of 100 fathoms, and an interval of 50 fathoms was used below 100 fathoms.

Fig. 2 shows the bathymetry of the area of interest. An outstanding bathymetric feature of Fig. 2 is Stonewall Bank which occupies the central part of the area and trends north 18° west as outlined by the 40-fathom contour line. The 30-fathom contour outlines three separate highs on the bank. The two southerly highs have the greatest relief and appear to be closely related. They are separated by a shallow east-trending submarine valley. The northern part of the bank has a less pronounced high that appears offset to the east compared to the general trend of the bank. Byrne (2, p. 65-74) stated that several ridges similar in size and shape are present on both sides of Stonewall Bank. From Fig. 2, it can be seen that ridges having the greatest

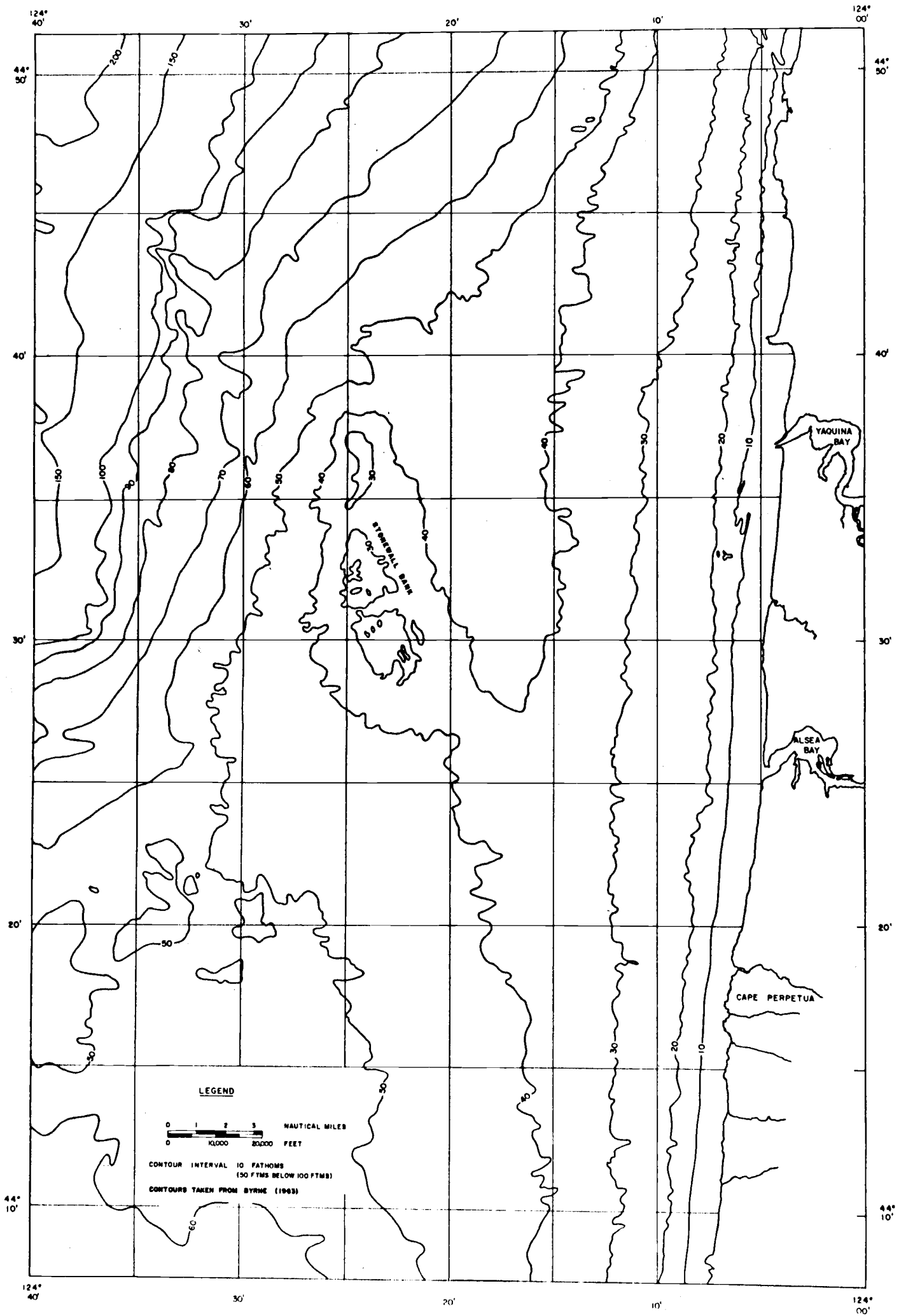


Figure 2. Bathymetric chart of the survey area

relief are present on the southern portion of the bank.

Immediately east of Stonewall Bank, between the bank and the Oregon coast, a broad valley exists that drains northward. Just north of the bank the valley is cut off by a slope that dips to the northwest. The floor of the valley has no major features and is relatively smooth. Fig. 2 shows that the deepest portion of the submarine valley lies closer to Stonewall Bank than to the shore line.

The bathymetry of the northwestern portion of the survey area consists of a fairly uniform slope dipping to the northwest. The dip of the slope increases with depth and is interrupted only by a set of northwest-trending ridges at about 100 fathoms.

The southeastern part of the area lies directly off Cape Perpetua. It has no distinct topographic features, a fact which is significant when compared to large variations of geophysical measurements that were made in the area. The ocean bottom of this area consists of a slope gently dipping to the west with the dip becoming steeper close to shore.

Southwest of Stonewall Bank, an unnamed shoal trending northeast is present. Part of the shoal is outlined by the 50-fathom contour. This shoal, herein named Acona Banks, may be structurally related to Heceta Bank which lies to the southwest of the survey area.

SEISMIC REFLECTIONS

The major part of the continuous Seismic Profiler or "sparker" work used in this paper was done in September of 1963. The instruments were mounted aboard the Research Vessel Acona of the Department of Oceanography, Oregon State University. Fig. 3 shows the track lines (dashed), along which seismic reflections were observed. Initially, northeast-bearing track lines were planned to be transverse to the major structural feature in the area, Stonewall Bank. Additional northwest-bearing lines, giving a grid coverage of the area, were made to resolve true dips and show any unsuspected structure. The spacing of the northeast-bearing lines was four nautical miles, and the spacing of the northwest-bearing lines was six nautical miles. These spacing distances were chosen because they were smaller than the dimensions of the structural features believed to be in this area, and they were consistent with considerations of time versus survey-area coverage.

Instrumentation

The sparker method is a specialized seismic reflection technique which provides a continuous profile of marine sub-bottom structure. Seismic reflections can occur at any acoustic interface within depth limits. If the reflections are of a sufficient energy level when reaching

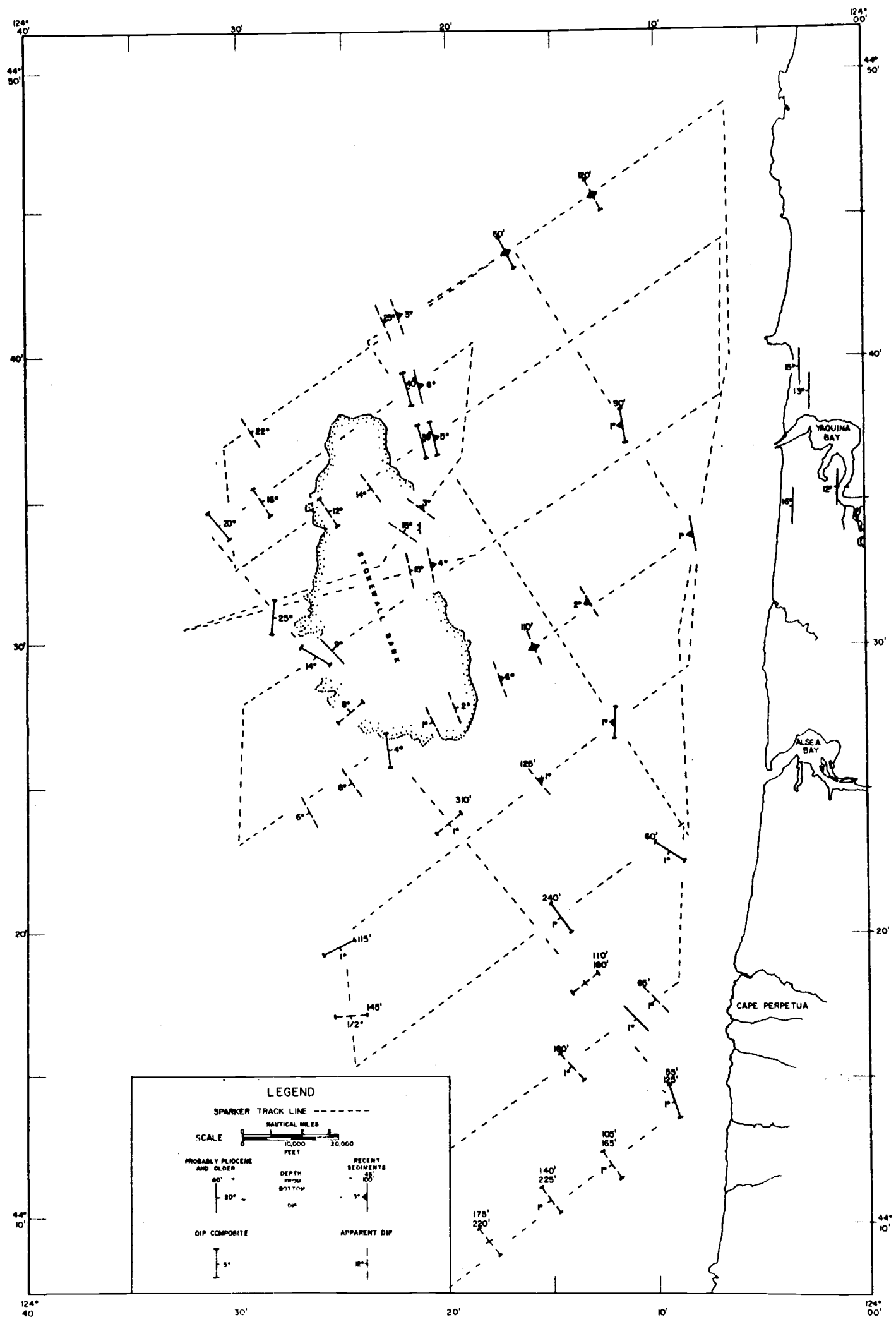


Figure 3. Seismic composite map of the survey area

the hydrophone, they are picked up and recorded by the system. The main components of the sparker are 1) spark power source, 2) spark trigger, 3) timing unit, 4) amplifiers and filters, and 5) recording unit. The following is a discussion of these components in the given order.

1. Spark power source: Sound energy is generated from the spark power source. In this component, a 60-cycle per second, 120-volt, alternating-current is passed through a heavy-duty transformer and rectifier circuit that charges two, one-microfarad capacitors at 1,200 volts. These capacitors are connected to two electrodes trailing in the water. At regular intervals, the capacitors are discharged across the electrodes creating an explosive spark in the water.

Marine Geophysical Services (8, p. 2) states that the spark generates energy of intermediate characteristics between that of a conventional echo-sounder and a seismic explosive. This energy approximates that of a blasting cap. Energy output is at a maximum between 250 and 900 cycles per second as compared to 10,000 to 20,000 cycles per second for conventional echo-sounders and 4 to 100 cycles per second for explosives.

2. Spark trigger: This component is mounted in the power-source cabinet and controls the rate of spark discharge with an air-gap switch. In the switch, a trigger

electrode momentarily ionizes the air with a spark between two high-voltage electrodes. This causes a discharge across the gap and allows the main current to pass from the large 1-microfarad capacitors to the electrodes trailing in the water.

3. Timing unit: The timing unit is located in the recorder and depends on the 60-cycle per second alternating-current power supply. The spark trigger is controlled by this unit and the discharge rate can be set from one discharge per 12 seconds to eight discharges per second. The timing unit controls 1) the rate and instant of spark discharge and 2) the rate and interval of recording.

4. Amplifiers and filters: A preamplifier, power amplifier, and band-pass filter are provided for two separate channels. Bias cutoffs in the power amplifiers limit the amplitude of signals that would otherwise burn the recording paper. Filters are usually set at band-pass frequencies of 75 to 200 cycles per second and 200 to 1200 cycles per second for the respective channels. The settings can vary for a particular area.

5. Recording unit: A dual-channel recorder, using helical-wire contacts and damp, electrolytic paper, presents the energy returns in a continuous profile on the recording paper. A good example of a sparker recording is given by McGuinness et al. (7, p. 222).

Operation Technique

During sparker operation, the noise level must be kept as low as possible. Some main sources of noise are cable pickup, ground loops, instrument microphonics, the survey ship, and ocean "whitecaps" caused by high winds. Any of these noise sources can be dominant, depending on the situation and conditions of operation. Care on the setup and upkeep of the various components of the sparker helped to reduce noise from the first three sources mentioned. Ship noise, minimized at slowest ship speeds (about three knots), was found to increase rapidly with speed to the point of masking many reflection returns at five to six knots.

A towing method has been adopted that amplifies both outgoing and incoming energy at a particular frequency. This method consists of towing the spark and hydrophone at a depth of one-quarter wave length of a desired frequency. The compressional wave form, assumed to be approximately sinusoidal with time and distance, is reflected at the air-water interface with a 180° phase inversion. At the depth of one-quarter wave length, the surface-reflected wave is in phase with the last half cycle of the compressional wave being emitted from the source, and the effects are additive. This procedure resulted in greater seismic energy received at the hydrophone from reflecting horizons.

Interpretation

Recordings from the sparker were handled according to a standard procedure. Ship position fixes were taken at 30-minute intervals, and the sparker records were marked at the fix time. The distance traveled during each 30-minute record section was measured from a map plot of the 30-minute navigation positions. An average ship velocity between the two stations was calculated using this distance and the 30-minute time lapse between stations. The average velocity was used for the computations in that particular interval.

Dip was computed using the straight ray-path assumption which seemed reasonable when the shallow depth of the reflecting horizons (0 to 400 feet below bottom) was considered. The equation for line dip computation (3, p. 137) is given by:

$$\phi = \sin^{-1} \frac{V\Delta T}{X}$$

where V is the average compressional wave velocity* in the medium at the depth of the event being considered, ΔT is the difference in one-way time of the seismic reflections at two close points on the surface where the same seismic reflection is recognized, and X is the ship distance

*Henceforth, the term velocity will be used to mean compressional wave velocity unless otherwise specified.

traveled between the two points.

Because energy reflects perpendicularly from a plane interface, the signals received from a sloping horizon do not originate directly beneath the ship. The transfer, or migration, of a sloping, record reflection to its proper spatial position is necessary. Horizontal migration distance can be calculated from the following equation (3, p. 137):

$$\underline{x} = \bar{V} T \sin \phi$$

where \underline{x} is the migration distance, \bar{V} is the average velocity from the surface to the event, T is the total one-way time to the event, and ϕ is the dip of the event. Migrations for this research were negligible and corrections were not applied to the data.

Sub-bottom velocities for the survey area were approximated using the exponential, velocity vs. depth equation from Nafe and Drake (9, p. 533). This equation was the result of seismic refraction work done in shallow water (less than 100 fathoms) off the Atlantic coast of the U. S. Values of velocity that were used in this research at given depths are listed in Table I.

TABLE I. DEPTH VS. VELOCITY

<u>Depth from Bottom</u>	<u>Velocity</u>
0-50 feet	5500 feet per second
50-150 "	6000 " " "
150-400 "	6500 " " "

The value of velocity undoubtedly varies horizontally due to a change in the type and consolidation of sediment, but because of a lack of velocity information in the survey area, no attempt was made to account for horizontal velocity variations.

A method for obtaining a maximum value of velocity in the sub-bottom structure using only a steeply dipping bed on a recording was used by the author. In the equation for the dip computation shown previously,

$$\sin \phi = \frac{V\Delta T}{X},$$

the value of $\sin \phi$ for steep dips comes close to one.

Since $\sin \phi$ can never be greater than one, any velocity used in the dip computation giving a value of $\sin \phi$ greater than one is invalid for that particular medium. Thus, the maximum velocity in a medium would be

$$\text{max. } V = \frac{X}{\Delta T}.$$

This equation, when used on a steeply dipping event in the survey area, gave a maximum velocity of 6100 feet per second at a depth of 100 feet; this velocity agrees very well with the values in Table I. The method is limited to shallow reflections where a straight ray-path assumption can be made.

Seismic reflections from small objects (such as large rocks) on the bottom, and beneath it, produce recordings which are sometimes confused with valid sub-bottom structure. They are characterized by hyperbolic-shaped events on the record. These hyperbolas become broader with depth. In many cases only one side of the curve may be present, leading to confusion with a dipping formation. The method used in this research as a means of hyperbola recognition was to construct the hyperbola corresponding to the respective depth and velocity of a questionable event. If the two curves compared in character, the reflection was considered questionable and assumed to be invalid.

Radar navigation was used for the survey; it provided an accuracy in position of \pm one-fourth nautical mile when close to shore (0 to 10 miles from the shore line). Class "A" LORAN and radar were used on the farther offshore tracks with an accuracy in position of \pm one-half nautical mile.

Seismic Reflection Results

Fig. 3 shows symbols for the generalized strike and dips of geological formations in the area of interest. Sub-bottom depths to the events are shown above these symbols. This presentation resulted from consolidation of the original data which were too numerous to present on a small map. First, the original events were classified

according to their quality as good, fair, and poor. Events graded "poor" were not used. Where a number of dip events with the same characteristics occurred in close proximity to each other, a single strike and dip symbol, marked with bars at the ends of the symbol, was used to represent all of the events in that group. The grouping, or composite, symbol represents data out to a radius of one nautical mile along the track lines. True dip and strike were computed at track-line crossings and corners. Reflections which occurred away from crossings and corners were plotted as apparent dips in the direction of the track lines and were represented by dashed symbols. A darkened triangular dip symbol was used to indicate layers that were believed to consist of unconsolidated or semi-consolidated sediments. The area of occurrence for this material was limited to the area between Stonewall Bank and the shore. The criteria used to differentiate between reflections from recent sediments and those from older rock were 1) calculated sub-bottom depth, 2) spatial relation to a structure of known age, such as Stonewall Bank, 3) uniformity of interpreted geological structure, and 4) magnitude of dip. The remaining symbols are of the normal type and indicate horizons that are believed to be older rocks.

Geological structural dips, shown along the coast (Fig. 3) around Yaquina Bay, were obtained from previous

work (17) and show dips of 12° to 16° to the west. In the area along the northeast side of Stonewall Bank, a continuous contact of older rocks, dipping 15° to 40° to the east, and recent sediments, dipping 3° to 6° to the east, is shown. A synclinal feature, with axis running north-south, was indicated by these opposing dips which border the area between Stonewall Bank and the Oregon coast. The syncline was still present at the northern limit of this seismic survey and its northern extent is not known. There was no seismic manifestation of the syncline south of the latitude $44^{\circ}25'$ N., and the gravity and magnetic data, shown later, supported the conclusion that this was its southern limit.

The east side of Stonewall Bank showed consistently eastward-dipping geological structure. The central portion of the bank has a cover of rocks which scattered the energy and made legible returns difficult to obtain. From the few reliable returns received in this central area, several dip reversals were observed which indicated that the bank is structurally complex. Seismic records from the southwestern part of Stonewall Bank also show dip reversals and one definite case of a minor anticlinal fold. The northwestern portion of the bank shows consistently eastward dips of about 20° . These data definitely show that Stonewall Bank is not a simple anticlinal or monoclinical structure. It is possible that the northern portion, having

consistent east dips on either side, is different from the southern portion, which has shallower and less consistent dips. Methods giving deeper penetration are needed to tell more of the bank's structure.

In the southern part of the survey area, south of 44°25' N. latitude, consistently strong reflections were observed. These horizons are horizontal or slightly dipping to the southwest and have depths from 0 to 300 feet below the ocean floor. Seismic records in this area often showed two reflections, indicated by two values for depth on the map (Fig. 3). The upper reflection is consistently smooth while the lower horizon, in two definite instances, is observed to have a non-smooth surface, which probably results from an unconformable contact at that depth.

A large number of events indicating sediment-filled channels or basins were observed in an area approximately six nautical miles wide along the entire survey-area coast. These events were not plotted in Fig. 3 because the track spacing was too wide to permit an outline of the channel or basin shapes.

GRAVITY

A free-air anomaly contour map of the survey area was compiled for this research using underwater and surface gravity meter data obtained by the Geophysics Research Group, Oregon State University. Gravity data along two profiles were analyzed by comparison with gravity that was calculated to result from two-dimensional, geological models constructed along the profiles. Calculation of the gravitational effect of the two-dimensional models was made using a method developed by Talwani et al. (15, p. 49-59). The models were adjusted within the limits of known data until their gravity effects were brought into agreement with observed gravity.

Free-air Anomaly Map

During July and August of 1962, a surface-ship gravity meter calibration range was established off Newport, Oregon (12, p. 1-11), where 149 gravity measurements were made at different locations using a Lacoste-Romberg underwater gravity meter. The accuracy of the stations was estimated to be \pm one mgal with a 90 percent degree of confidence. The area of the gravity range is bounded by the latitudes $44^{\circ}10'$ to $44^{\circ}50'$ N. and longitudes $124^{\circ}07'$ to $124^{\circ}20'$ W. Surface gravity measurements were made at sea using a Lacoste-Romberg surface-ship gravity meter off the entire

Oregon coast in the spring of 1963. One line of surface-meter data was used in this research. A portion of this line along which underwater-meter data were obtained gave gravity values between one and six mgal higher than adjacent underwater-meter values whose accuracy is \pm one mgal (Dr. P. C. Dehlinger, personal communication).

Fig. 4 is a free-air gravity anomaly map of the survey area at sea level. The underwater gravity stations are shown as solid circles, squares, and triangles, depending on the accuracy of the data. The surface-meter stations are shown as open triangles. The contour interval for the free-air map is five mgal. The dashed lines represent contours based on surface-ship data which are less reliable than the underwater data.

Lines A-A' and B-B', shown in Fig. 4, indicate the profiles along which the measured gravity was compared with gravity that was calculated from assumed geological cross sections. The lines were placed to cross the two outstanding features shown by the map--a gravity high off Cape Perpetua and a broad north-south gravity low off Newport.

Terrain effects were considered before any gravity computations were made using assumed geological structure. Underwater meter readings were made on the sea floor so terrain corrections were applied at the underwater locations even though the stations were raised to sea level.

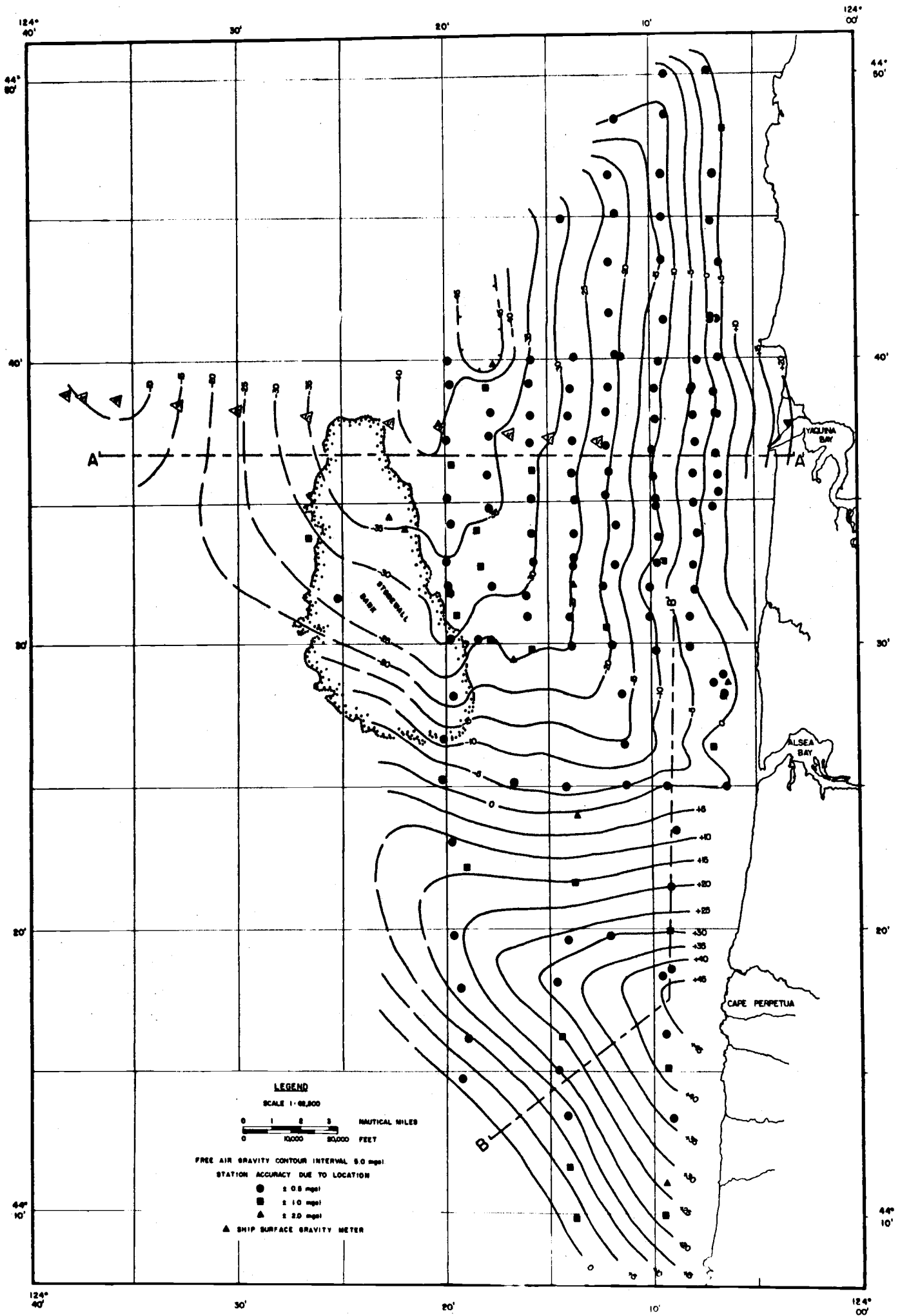


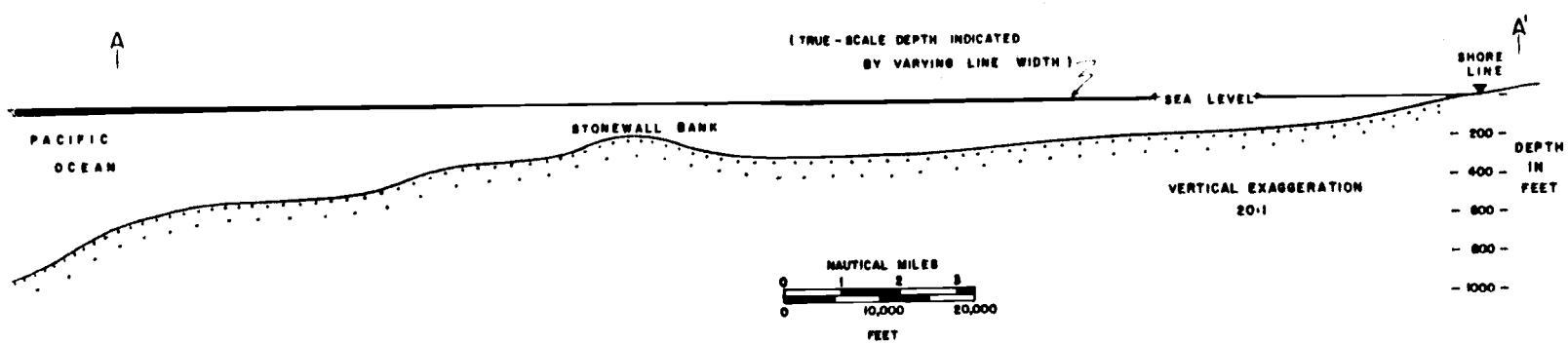
Figure 4. Free-air gravity anomaly chart of the survey area

Surface-meter readings were affected by terrain to a lesser degree, because of their distance from the sea floor, than underwater readings.

Maximum bottom relief occurred along section A-A', so maximum terrain corrections were expected here. Part a of Fig. 5 shows the bottom topography of A-A' in a 20:1 vertical exaggeration with the true scale relief shown in dark outline. To approximate the terrain effects, the cross section was divided into a series of simple, two-dimensional shapes which approximated the bottom relief. The terrain corrections for these two-dimensional shapes were then calculated using a series of standard curves (6, p. 226-254), and the effects of these simple shapes were summed along the cross section. In all cases where approximations were made, they were made in favor of excessive gravity corrections in order to give a maximum possible correction. Part b of Fig. 5 shows the maximum terrain correction as the cross-hatched area corresponding to the bottom relief shown in Part a of the same figure. At no point was the correction greater than 0.2 mgal. The terrain corrections, being much smaller than the gravity range accuracy, were neglected in the consideration of gravity in the survey area. Three-dimensional terrain corrections were calculated, using tables from Hammer (4, p. 184-194), on the end points of line A-A' to

PART a

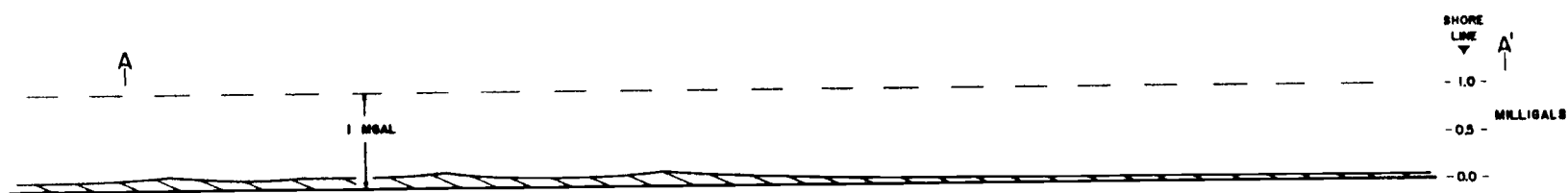
BOTTOM RELIEF ALONG LINE A-A'



PART b

LINE A-A'

MAXIMUM TERRAIN CORRECTION



PART c

LINE A-A'

FREE-AIR AND BOUGUER ANOMALIES

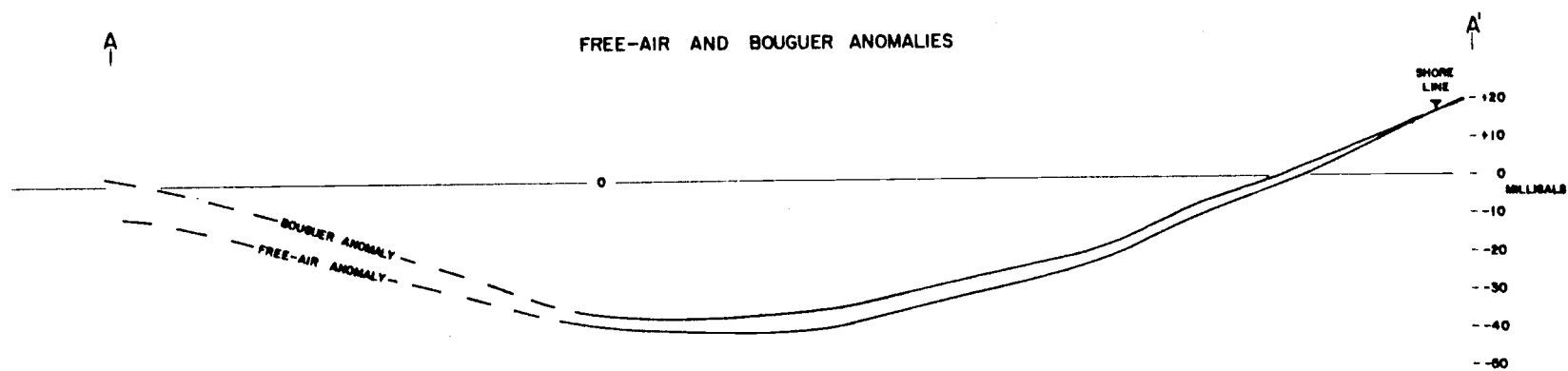


Figure 5. Bottom topography, terrain correction, and gravity of line A-A' (see Fig. 4)

determine the effect of a changing regional slope along A-A'. Corrections were made to a radius of 12 nautical miles and gave values of 0.25 mgal on the seaward end of A-A' and 0.35 mgal on the shore end. The difference in these values was small and did not affect the consideration of local gravity along A-A'. A rock density of 2.1 gm per cm³ was used for all terrain corrections.

An important factor to take into consideration when discussing gravity in the survey area is the effect of a regional gravity variation, resulting from the continental-oceanic crustal change, on gravity variations resulting from local structures. Gravity along B-B' will not be greatly affected since it mainly parallels the coast, but line A-A' runs east-west and gravity values may be significantly altered by the crustal change. Fig. 6 shows the free-air anomaly of line A-A' in relation to a surface-meter track extending farther out to sea. The gravity along this profile is complex, and to account for regional variation of gravity would require knowing the general nature of the crustal structure in this area. The effect of a regional gravity decrease to the west would distort the local gravity so as to make it appear lower to the west than it would be from effects of local geological structure alone. This would deepen the gravity model of a geological feature, such as a syncline, and skew it to

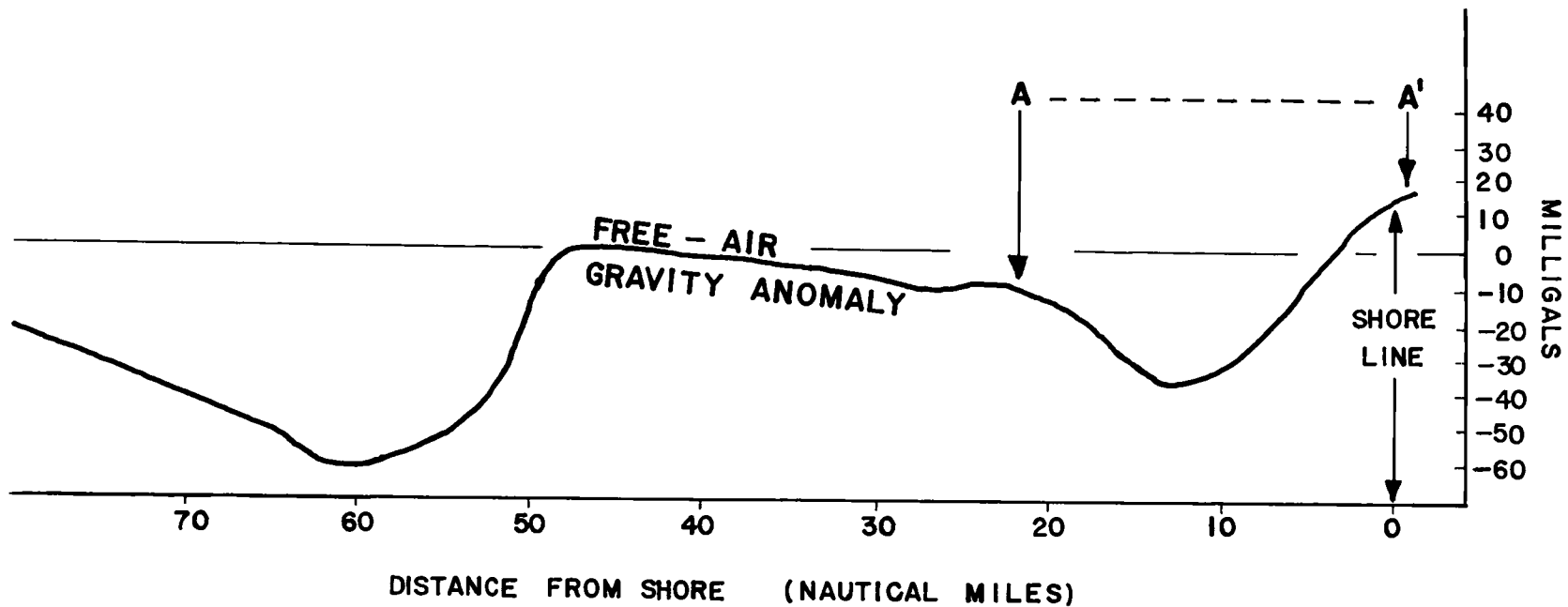


Figure 6. Free-air gravity anomaly extending from shore line to 70 nautical miles along latitude $44^{\circ}35'$ N. (This profile is along interpretative line A-A'.)

the west with depth. The effect of a regional gravity increase to the west would have the opposite effect.

Cross Section A-A'

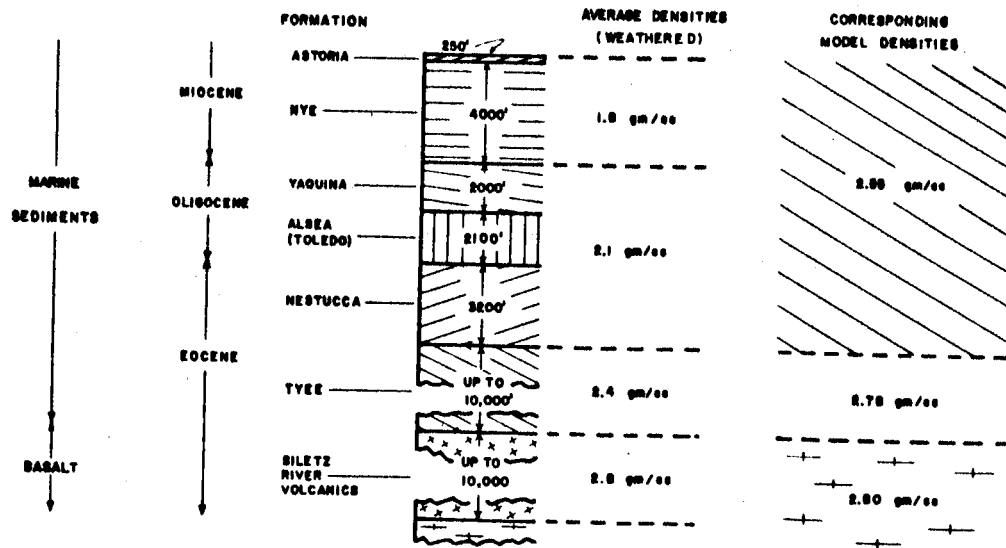
Line A-A' (see Fig. 4) was placed across the large gravity low in the northern portion of the survey area so that it crossed normal to the gravity contours. It extends outside the gravity range along a surface-meter track where the direction of gravity contours is less certain. The development of a section along line A-A' is discussed in the following sections under Bouguer anomaly, two-dimensional model development, and results.

Bouguer Anomaly. The Bouguer anomaly is commonly used to compare gravity measurements at a datum, usually sea-level. Observed gravity is corrected with free-air, Bouguer, and terrain corrections which make all gravity measurements comparable by theoretically placing all gravity stations at a constant elevation on a smooth earth. Variations in the density columns beneath the observation points show up as variations in the corrected gravity. For gravity stations at sea, corrections are first applied to the free-air gravity for terrain variations of the sea floor so as to make the sea floor flat, and then the sea water is theoretically replaced with rock of a given density by applying the Bouguer correction. Bouguer gravity anomaly was calculated over the assumed geological

cross section along A-A' using sea level as the datum surface. This simplified computations in that the water did not have to be considered in the geological model. A density of 2.10 gm per cm³ was used for the replacement rock and 1.03 gm per cm³ was used for sea water. Geological data supporting the value for rock density are presented later. Part c of Fig. 5 shows both the free-air and Bouguer anomalies along line A-A'.

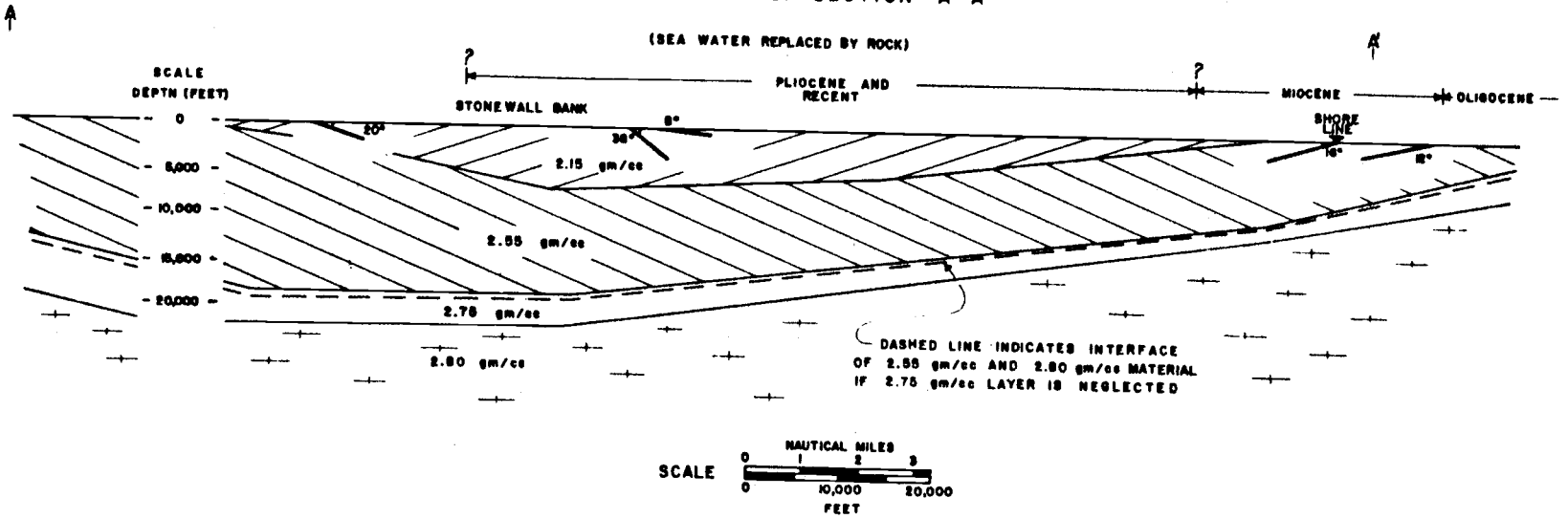
Two-dimensional Model Development. An initial two-dimensional model was constructed along line A-A' by 1) extrapolating shore data seaward, 2) using seismic data in the area, and 3) using rock samples taken from Stonewall Bank. This model was used for the beginning of gravity computations. Geology in the Newport area consists of a west-dipping, coast embayment of Tertiary sediments. A columnar section of the formations and their thicknesses in this area is shown in Part a of Fig. 7 (John P. Lenzer, personal communication). Corresponding geologic ages of the formations are shown to the left of the columnar section, and the ages of the surface outcrops in relation to their horizontal positioning on A-A' are shown above the model in Part b of Fig. 7. As it is indicated in Part b, the western extent of the Miocene is unknown but is assumed to terminate immediately offshore with the onset of Pliocene sediments.

DENSITY COLUMNAR SECTION OF YAQUINA BAY AREA



PART b

DENSITY MODEL OF SECTION A-A'



PART c

LINE A-A'

CALCULATED AND BOUGUER ANOMALIES

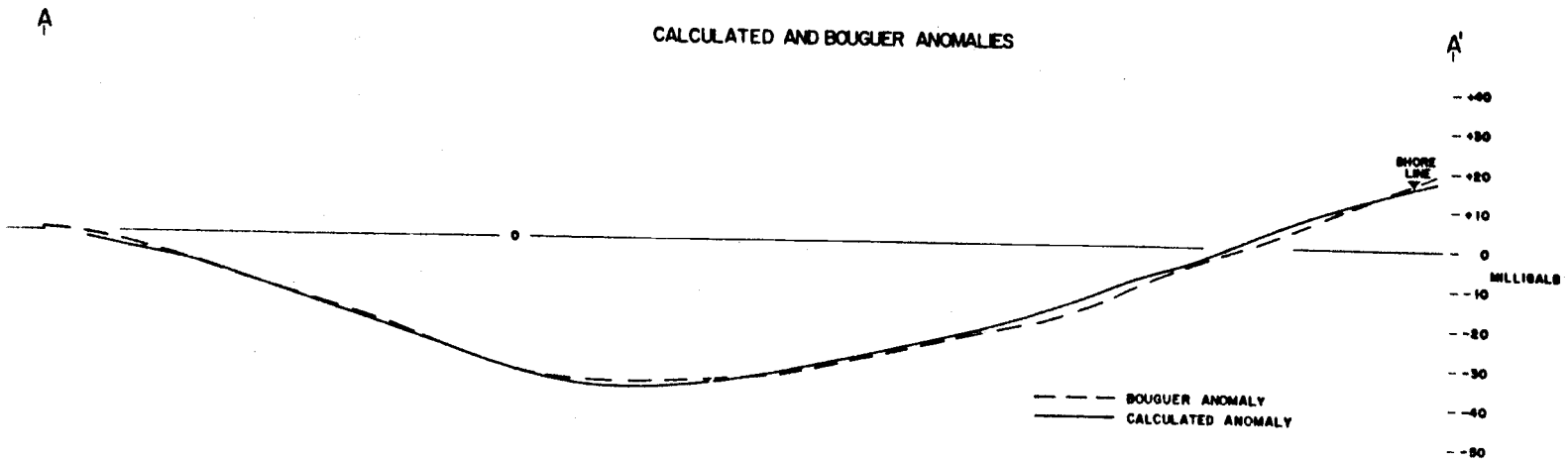


Figure 7. Geology, interpretative geological model and gravity along line A-A' (see Fig. 4)

Average density values for rock (14) from the Tertiary section, are shown adjacent to the columnar section of Part a, Fig. 7. The densities of these rocks were measured from air-dried surface samples, some of which were slightly weathered. Due to water saturation and depth of burial, the densities of clastic sediments in the section are undoubtedly higher at depth than the measured densities. Four density divisions were established for purposes of this research: 1) The upper division was assumed to consist of Pliocene and Upper Miocene rocks, which have no counterpart in Part a, Fig. 7. It was assigned a density of 2.10 gm per cm³ and was used for the Bouguer correction. The density was chosen by using the average density of the youngest measured rocks, Miocene sedimentary rocks at 1.9 gm per cm³. Since these rocks were dry, the density was increased to a density of 2.10 gm per cm³ to account for water saturation. 2) A second division was formed consisting of rocks from Late Eocene through Oligocene to Middle Miocene. Since these rocks were shown to have densities of 2.0 gm per cm³ at the surface (Part a, Fig. 7), their density at depth was made higher, about 2.4 to 2.5 gm per cm³. 3) A third division was made for Middle Eocene rocks whose surface densities average 2.4 gm per cm³. Density for this division was assumed to be 2.6 to 2.7 gm per cm³. 4) The fourth division included all rocks of Early Eocene

or older age and was considered basement rock for the model. This division's density was made 2.80 gm per cm³, a value supported by the density data for crystalline rock in this area.

Dips were selected from areas along section A-A' on the seismic composite map (Fig. 3) where it was felt the shallow sub-bottom structure was reliably known. At the east end of section A-A', west dips from 12° to 16° are shown on Part b of Fig. 7. In the Stonewall Bank area, an east dip of 20° is shown on the west side of the bank and east dips of 40° and 6° are shown on the east side of the bank. The 6° dip was believed to be either from recent sediments or from a contact between recent sediments and older rocks. Dips are plotted on the model's upper surface on Part b, Fig. 7. Density-division interface positions were determined by projecting the shore formation contacts parallel to the dips.

Rock samples (Neil J. Maloney, personal communication) have been dredged from Stonewall Bank and the surrounding area by the Department of Oceanography, Oregon State University. Results from the study of these samples show that: Stonewall Bank consists mainly of Pliocene rocks which are in the first density division of the model, and the west side of the bank is older than the east from the evidence of a Late Miocene sample dredged from the north-

west side of the bank. From these data it was reasoned that the interface between the first and second density divisions should outcrop on the bottom west of Stonewall Bank.

The initial model, similar to that of Part b, Fig. 7, was developed into a broad syncline conforming to the preceding data and reasoning. For calculations, a density of 2.80 gm per cm³ was subtracted from all four density divisions making the density of the fourth division, or basement rock, zero and eliminating the need for the fourth division's gravity calculation. Gravitational attraction for each of the three remaining density divisions was computed separately and their effects were added, resulting in a calculated gravity anomaly along line A-A'. Since all of the basement rocks surrounding the model were removed in the computations, the magnitude of the calculated anomaly was increased to account for the missing basement attraction. For convenience, this was accomplished by raising the calculated anomaly curve so that its gravity agreed in magnitude with the Bouguer anomaly at one particular station that was chosen just offshore on line A-A'. The calculated anomaly was then compared to the Bouguer anomaly and the model dimensions and densities were adjusted to produce a closer fit between the calculated and observed gravity always staying within the limits

imposed by the geological data. After several adjustments and computations of the model, a final two-dimensional model (Part b, Fig. 7) was obtained.

Results. The calculated anomaly for the final model is shown by a solid curve in Part c, Figure 7, and the Bouguer anomaly is shown as a dashed curve for comparison. Maximum deviation between the Bouguer and calculated anomalies is three mgal. The model solution is, of course, not unique; there are a number of shapes and combinations of densities that would produce the same gravity configuration. It is felt, however, that the seismic and geologic control has eliminated the majority of these variations and has enabled the construction of a model reflecting the density distribution to a reasonable degree of accuracy.

The final two-dimensional model, Part b of Fig. 7, shows a broad synclinal feature. The axis of the syncline at shallow depths is between Stonewall Bank and the shore, as indicated by seismic data, and shifts west to a position beneath Stonewall Bank at depths of 19,000 to 21,500 feet. This axis shift would indicate a thickening of the assumed Tertiary sediments to the west. If the regional gravity were found to decrease linearly to the west, the interpretative model would be shallower and the synclinal axis would not shift as much to the west with depth.* An

*As an example of the effect of regional gravity on

increase to the west would produce the opposite effect on the model. No broad anticlinal feature is seen in the area covered by section A-A' (minor anticlinal folds, as mentioned previously are definitely present in the Stonewall Bank area).

One alternative to the model along A-A' is to remove the third layer of 2.75 gm per cm³ rock and replace it with the basement rock. When this is done and the resulting model is recalculated, a shallower basement is obtained shown by the dashed line in Part b, Fig. 7. This does not lower the bottom of the 2.55 gm per cm³ material by a significant amount.

Because of less control, the portion of the model west of Stonewall Bank is not considered as reliable as that to the east. In all parts of the model it must be recognized that assumed density contrast lines usually do not coincide with geological formation boundaries.

the model of Part b, Fig. 7, a regional correction approximation was made using the gravity of Fig. 6. A maximum, linear regional gradient was computed from Fig. 6 to be 0.266 mgal per nautical mile decreasing to the west. This gave a regional gravity correction at the position of Stonewall Bank of + 3.9 mgal with respect to shore. A simple Bouguer correction for this gravity change was applied to the model using the density contrast of 0.25 gm per cm³ (difference between basement rock density of 2.80 and sedimentary rock density of 2.55 gm per cm³). The basement of the model at the position below Stonewall Bank was raised approximately 1300 feet by the correction.

Cross Section B-B'

In the southern part of the survey area, a large gravity high is evident near the coast of Cape Perpetua. It extends with decreasing intensity to the west and northwest. Line B-B' (Fig. 4) was placed normal to the gravity lines by breaking B-B' into southwest-bearing and north-bearing lines because of the two-dimensional assumption used in model calculations. The cross section along B-B' is discussed in the following sections under Bouguer anomaly, two-dimensional model development, and results.

Bouguer Anomaly. A Bouguer-type anomaly for section B-B' was computed for a datum at an elevation of -130 feet instead of sea level as along A-A'.* This was done because all of the original gravity readings were made on the bottom. Hence, a horizontal datum plane with close agreement to bottom depths was used to keep density assumptions to a minimum. This depth was 130 feet. The Bouguer anomaly in B-B' had all material above the datum removed and all space below the datum filled with rock of 2.10 gm per cm³ density. This density was chosen assuming the upper few feet (0-20 feet) of sub-bottom structure consisted of recent

*When used in reference to the gravity along B-B', the term Bouguer anomaly will henceforth mean the gravity anomaly resulting from the corrections discussed in this section.

sediments* similar to those along line A-A'. The Bouguer anomaly along line B-B' is shown on Part a of Fig. 8.

Two-dimensional Model Development. The outstanding geological feature in the southern part of the survey area is Cape Perpetua. It consists of a complex development of igneous intrusives and flows causing a prominent headland on the Oregon coast. The Cape shows no extension in submarine topography offshore where the bottom is relatively smooth. Seismic data in this area show nearly horizontal, strong reflectors at relatively shallow depths. No reflections were seen below these arrivals. Geological data are sparse in the area of line B-B', and there is no indication of deep structure except that inferred from Cape Perpetua. Since the gravity high in this area centers off the Cape, a complex igneous body, and is obviously related to it, the structure resulting in the high should be igneous in nature.

The Bouguer gravity anomaly along B-B' was used to determine the shape of the anomalous crystalline structure at depth. Due to the non-uniqueness of mathematical solutions for the gravitational attraction of mass distributions, an infinite number of shapes and densities for the subsurface mass is possible. Two basic configurations considered most likely are shown in Parts b and c of

*Bottom samples show no rocks in this area as yet (Neil J. Maloney, personal communication).

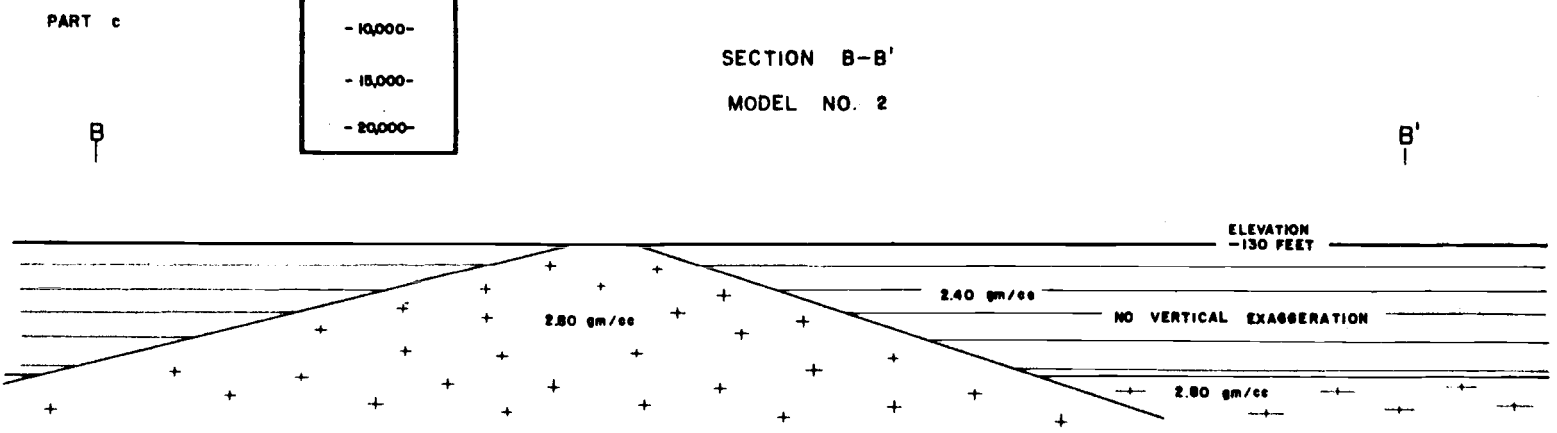
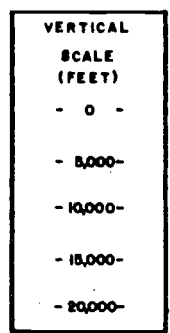
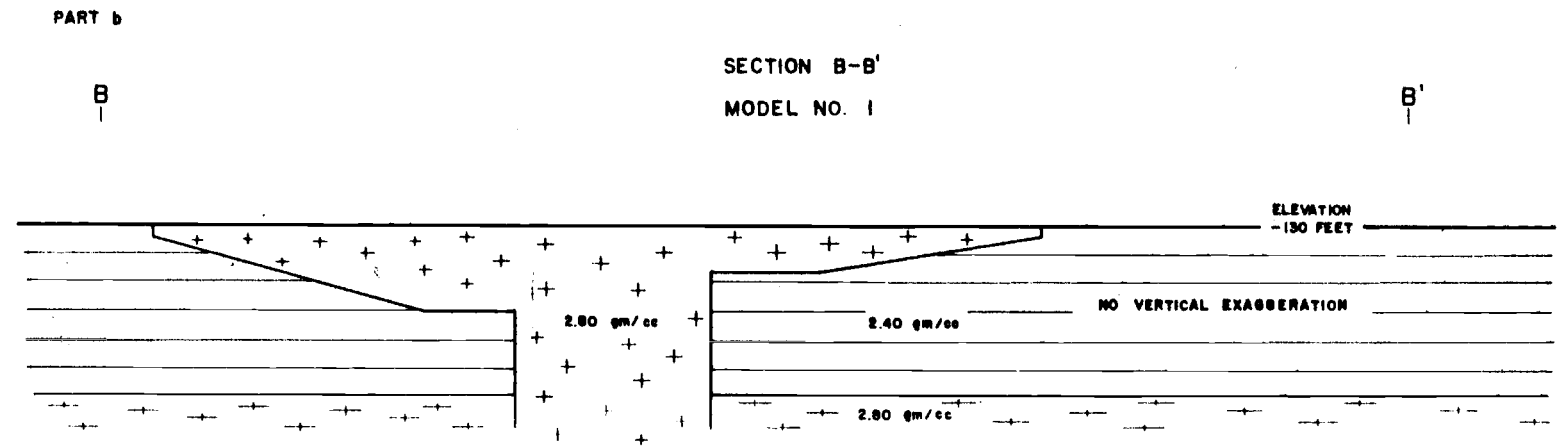
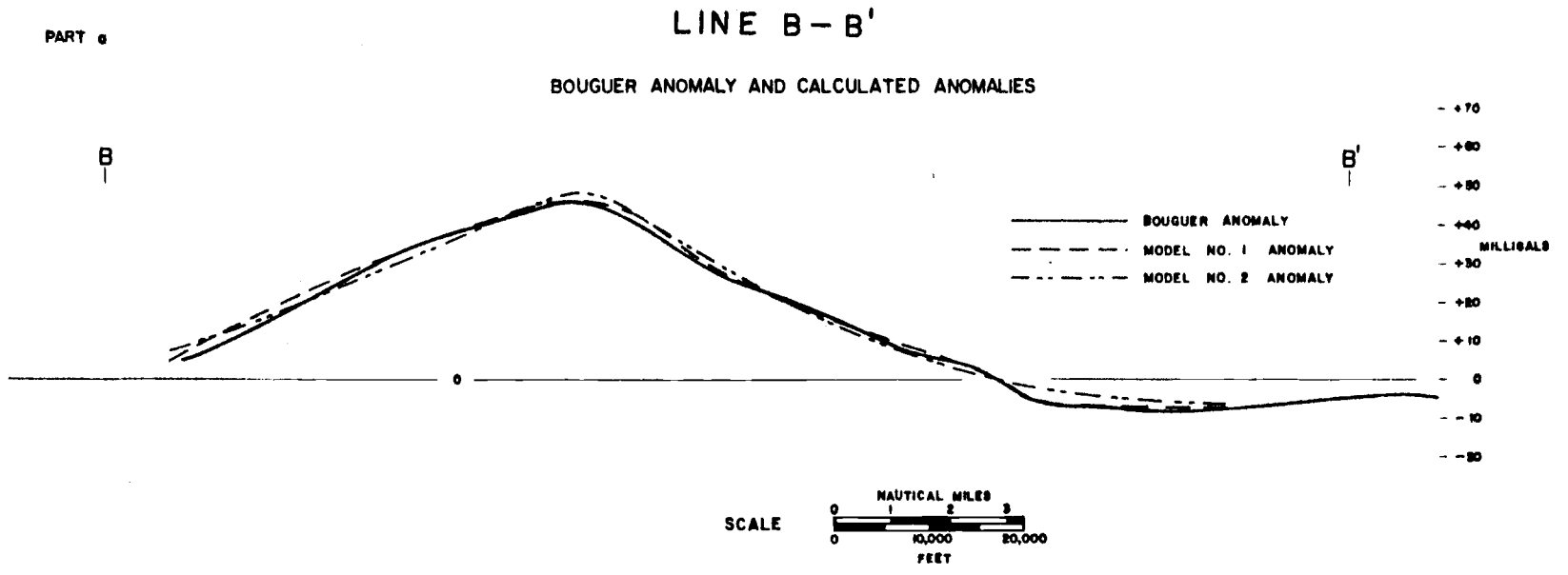


Figure 8. Observed and calculated Bouguer gravity anomalies and interpretative geological models along line B-B' (see Fig. 4)

Fig. 8. For the crystalline rock density of these configurations, igneous rock data indicate that 2.80 gm per cm^3 is the best choice, and this density was used for calculations. Density values for the country rock surrounding the configurations was first chosen to agree with rock from the syncline to the north. To achieve these values, line B-B' was extended north until it intersected line A-A'. At this intersection point, a sedimentary section of 12,000 to 13,000 feet with a density of 2.55 gm per cm^3 was encountered. This density was initially used for country rock of the section along B-B' but was changed to 2.40 gm per cm^3 to make the calculated, model anomaly compare more favorably with the measured anomaly.

Results. The final models are shown in Parts b and c of Fig. 8. Calculated anomalies for these models are shown in comparison to the Bouguer anomaly in Part a, Fig. 8. Gravity from the final models was brought to an agreement of better than four mgal with the Bouguer anomaly. Model 1 resembles a deep, vertical intrusive capped with broad, thick flows near the surface. Model 2 appears as either a rounded intrusive or a buried cone. The configuration of Model 2 is the simpler of the two models and lends itself readily to reproducing the Bouguer anomaly with the least effort. Shallow volcanic flows, not extensive in thickness, could be present in either model; they could

cause the seismic reflections but not have enough mass to affect gravity appreciably. The final density for the country rock in the models is 2.40 gm per cm³ (Parts b and c, Fig. 8). This density was chosen because it agrees closely with the corresponding density in the section along A-A' and gives basement depths of 13,000 to 16,000 feet on B-B' compared to that of 12,000 to 13,000 feet on A-A' at the intersections of the two lines.

MAGNETICS

During 1963 and 1964, measurements of the earth's magnetic field were made in the offshore Oregon area by the Geophysics Research Group of the Department of Oceanography, Oregon State University. A nuclear precession, total-intensity, magnetometer was used in conjunction with the Research Vessel Acona for the majority of the work. As a check on the accuracy of the magnetometer data, five positions were used in the survey area (Fig. 9) where track lines intersected. At these intersections, magnetic intensity values were taken from the records and are compared in Table II.

TABLE II. MAGNETIC READING COMPARISONS AT TRACK INTERSECTIONS

<u>Track Line Magnetic Values (gammas)</u>	<u>Difference (gammas)</u>
55040-55015	25
54910-54885	25
54930-54865	65
54705-54675	30
54470-54440	30

Disagreement varies from 25 to 65 gammas with an average of 35 gammas. The error is believed to be due mainly to 1) navigation, which was done using LORAN and radar positioning and 2) diurnal variations of the earth's magnetic field which averages as high as 30 gammas per day in the summer. The nuclear precession magnetometer is believed

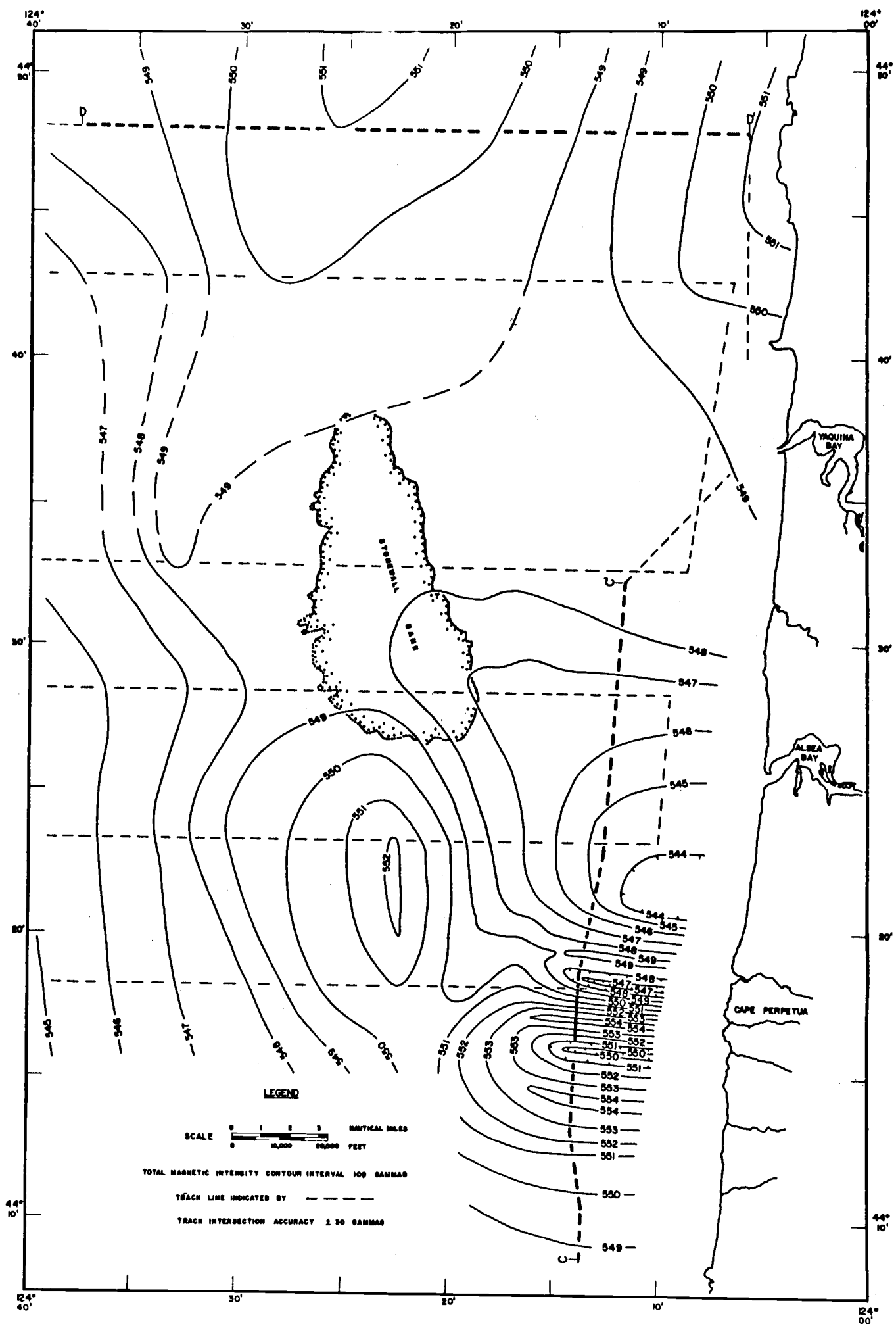


Figure 9. Total magnetic intensity map of the survey area

to have an accuracy of \pm five gammas. The recording of magnetic intensity was continuous so that intensity gradients were not as dependent on accurate navigation as plotting of magnetic contours.

Data from tracks in the survey, where track spacing is approximately five nautical miles, were contoured with a 100-gamma contour interval in Fig. 9. Contours were dashed where track spacing was greater than five nautical miles. In the southeastern part of the survey area, magnetic intensity gradients are large and contouring may be subject to error due to lack of sufficient data to define the contours more accurately.

Fig. 10 shows two magnetic cross sections that were chosen along C-C' and D-D' (Fig. 9). Computations of depth and interpretations were made along the sections using methods that assumed the anomalies resulted from two-dimensional dikes.

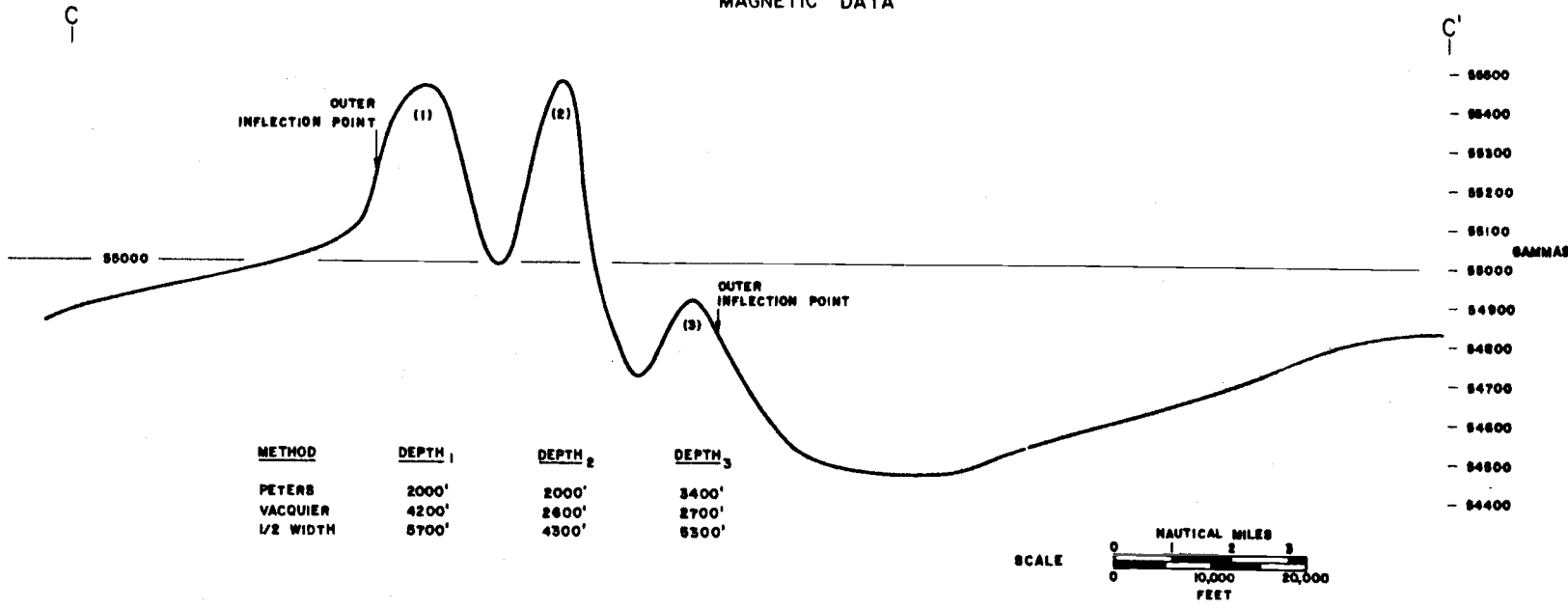
Section Along C-C'

The large anomaly along C-C' lies directly off Cape Perpetua and is assumed to have its long axis in the east-west direction as indicated by the gravity data (Fig. 4). Since it is doubtful that the single magnetic track line (along C-C') crossed the body exactly at right angles, all measured gradients are assumed to be less than or equal to their maximum value. The magnetic intensity reaches highs

PART a

LINE C-C'

MAGNETIC DATA

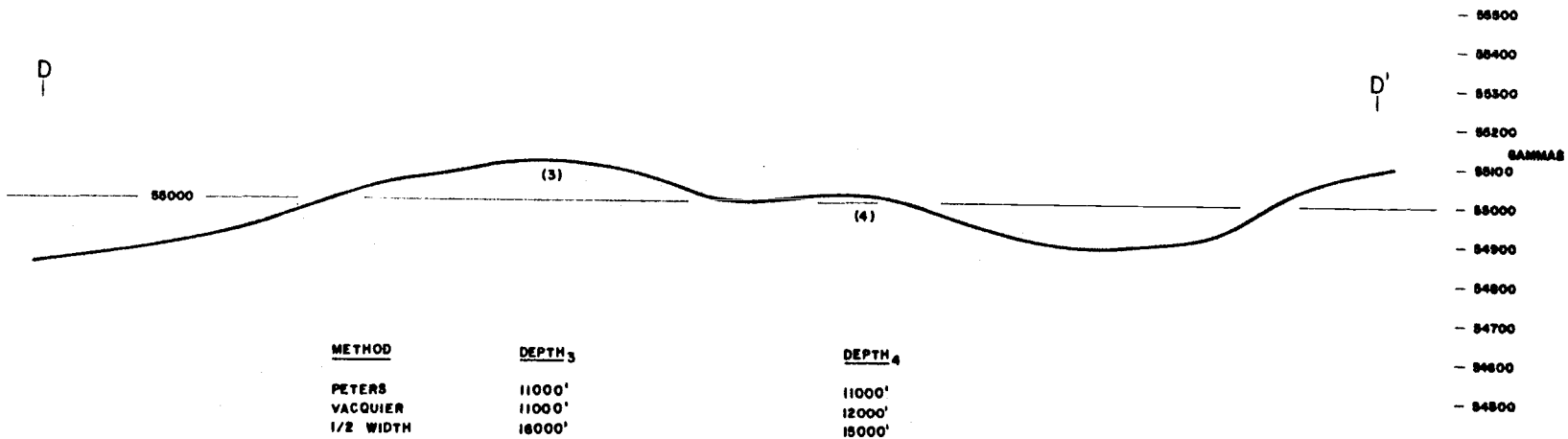


METHOD	DEPTH ₁	DEPTH ₂	DEPTH ₃
PETERS	2000'	2000'	3400'
VACQUIER	4200'	2600'	2700'
1/2 WIDTH	5700'	4300'	5300'

PART b

LINE D-D'

MAGNETIC DATA



METHOD	DEPTH ₃	DEPTH ₄
PETERS	11000'	11000'
VACQUIER	11000'	12000'
1/2 WIDTH	16000'	15000'

Figure 10. Magnetic sections along C-C' and D-D' (see Fig. 9)

of 55,470 gammas and lows of 54,460 gammas. Because of large gradients and high intensities of the magnetic field, the anomaly in this area is believed to result from a relatively shallow mass of crystalline rock.

For interpretative purposes, it was necessary to determine whether the anomalies resulted primarily from the shape or the internal inhomogeneities of the crystalline rock mass. Susceptibilities of crystalline rocks vary greatly especially if they have a history of thermal and mechanical alterations. Cape Perpetua rocks are of this type. The breadth of the low on the north side of the anomaly indicates an extensive body, and the narrow, sharp peaks on the anomaly indicate small dimension bodies. From these considerations it was believed that the crystalline mass is a broad body containing areas of large magnetic susceptibility changes. Since the inclination of the earth's magnetic field is 70° north in this area, lows would be expected on the north side of anomalous masses if they were magnetized in the direction of the earth's present magnetic field. It was assumed that the broad magnetic low on the north of C-C' was due to the broad crystalline mass, and the alternate peaks and lows on the anomaly were due to susceptibility changes within the larger mass. Gradients of these sharp peaks were used for depth calculations which assume the body is a two-dimensional dike with sharp corners. There are two main factors that cause

depth calculations to overestimate depths: 1) track lines crossing magnetic anomalies at other than right angles as mentioned previously and 2) the absence of sharp corners of the anomalous body. Both of these effects reduce the magnetic gradients. It is evident that calculations probably give only a maximum depth value and actual depths can be shallower.

Peters' "slope" method (11, p. 310-311) was the first to be used in this study. Depths obtained for the three peaks, indicated in Part a, Fig. 10, were 2,000 feet, 2,000 feet and 3,000 feet. A single pole, one-half width, depth rule (5, p. 381-383) was the simplest estimation of depth using the assumption of vertical intensity. Application of this method to the three peaks gave depths of 5,700 feet, 4,300 feet and 5,300 feet.

The two previous methods assumed that the measured magnetic intensity was vertical only. Since total intensity was measured, a method that deals with total intensity published by Vacquier et al. (16, p. 1-10) was applied to the data. In the publication, magnetic anomalies were computed from models and were compared to the model structure. These models represent the magnetic effect due to rectangular prisms having horizontal tops and extending infinitely downward with vertical sides. The models show that the zero curvature, or inflection, points on the

magnetic intensity map are most useful in locating the edges of rock bodies. The depth of the anomalous body can be estimated from the distance between curvature maxima or minima and the zero curvature points. Depths obtained by this method from the three peaks on line C-C' are 4,200 feet, 2,600 feet and 2,700 feet. The inflection points, indicating the edges of the anomalous body, are shown (Part a, Fig. 10). The northern edge of the body, indicated from the inflection point along C-C', is not consistent with Model 1 (Part b, Fig. 8) of the gravity section B-B'.

Results of depth computations using the three methods are given in Part a of Fig. 10.

Section Along D-D'

An anomaly high directly north of Stonewall Bank in the extreme northern part of the survey area was chosen for depth calculations. The magnetic measurements taken along the northernmost east-west track line (Fig. 9) were used to plot a magnetic section along D-D' as shown in Part b of Fig. 10. The magnetic intensity varies from 54,870 to 55,100 gammas. The magnetic intensity high in this area continues southwest to the west of Stonewall Bank. Depth computations were done in the same manner as those in the previous section with the exception that the 70° declination of the earth's magnetic field was not

accounted for in the east-west cross section. Calculations were made with two peaks indicated by (4) and (5) on the anomaly of Part b, Fig. 10. Peters' "slope" method gave depths of 11,000 feet and 11,000 feet. The single pole, one-half width, depth rule gave 16,000 feet and 15,000 feet. Vacquier's total intensity method gave 11,000 feet and 12,000 feet for depths. Because of the good agreement of Peters' and Vacquier's methods, the depth to basement is believed to be close to 11,000 feet.

South of line D-D', magnetic intensity variations are very small in the gravity synclinal area (Fig. 4) around Stonewall Bank, and no large anomalies are present. This would seemingly support the existence of a deep basement in this area as deduced from gravity.

SUMMARY AND CONCLUSIONS

The portion of the survey area north of latitude $44^{\circ}25'$ N. is believed to consist of a large syncline whose east side and south end are outlined by gravity (Fig. 4). From shallow seismic data (Fig. 3) and the shape of the free-air gravity anomaly along the Oregon coast, the syncline is believed to run in a north-south direction. A geological two-dimensional model (Part b, Fig. 7) that was constructed to agree with the observed gravity and geological data along A-A' (Fig. 4) gives synclinal basement depths of 19,000 to 21,500 feet. At shallow depths in the model, the synclinal axis is between Stonewall Bank and shore as indicated by seismic data. The model's synclinal axis then shifts to the west with depth indicating a thickening of sediments with depth. If regional gravity decreases to the west along A-A', the model would have to be made shallower and the axis shift to the west with depth would be less pronounced. Seismic data indicate complex minor folding and possible faulting on the central and southern portions of Stonewall Bank. The southern limit of the syncline is believed to be outlined by a rise in gravity values near $44^{\circ}25'$ N. latitude (Fig. 4). The northern limit of the syncline is unknown, but magnetic data (Fig. 9) indicate that the basement rises to the north where depth computations (Part b, Fig. 10) give

depths of about 11,000 feet. Gravity and magnetic highs (Figs. 4 and 9) in the far western-central part of the survey area indicate a rise in the basement and a possible anticlinal structure to the west of Stonewall Bank.

The portion of the survey area south of latitude $44^{\circ}25'$ N. is believed to consist of a large crystalline rock mass outlined by gravity and magnetic data (Figs. 4 and 9) off Cape Perpetua. These data contours indicate that the crystalline mass noses down to the northwest. Two geological, two-dimensional models (Parts b and c, Fig. 8) were constructed across this mass along B-B' (Fig. 4) to agree with observed gravity data. The models are surrounded by sedimentary country rock with basement depths of 13,000 to 16,000 feet. Model 1 (Part b, Fig. 8) was eliminated by magnetic data leading to the conclusion that the crystalline rock mass is some form of Model 2 (Part c, Fig. 8). Depth computations from magnetic data (Part a, Fig. 10), five nautical miles off Cape Perpetua, placed the top of the crystalline mass at a depth less than about 3,000 feet. Shallow seismic reflections occurring as doublets in the southern area indicate an upper layer resting unconformably on the lower rock. This upper layer may be volcanic flow rock.

The results of this geophysical study indicate that geological structures along the coast near Newport, Oregon,

probably do continue to the west although this may not always be in evidence from the sea floor geology. In such cases, geophysical studies such as those conducted in this research can be utilized to extend coastline geology seaward.

BIBLIOGRAPHY

1. Backus, Milo M. Water reverberations--their nature and elimination. *Geophysics* 24:233-261. 1959.
2. Byrne, John V. Geomorphology of the continental terrace off the central coast of Oregon. *Ore Bin* 24:65-74. May, 1962.
3. Dobrin, Milton B. Introduction to geophysical prospecting. 2d ed. New York, McGraw-Hill, 1960. 446 p.
4. Hammer, Sigmund. Terrain corrections for gravimeter stations. *Geophysics* 4:184-194. 1939.
5. Heiland, C. A. Geophysical exploration. New York, McGraw-Hill, 1946. 1013 p.
6. Hubbert, M. K. Gravitational terrain effects of two-dimensional topographic features. *Geophysics* 13:226-254. 1948.
7. McGuinness, W. T., Walter C. Beckmann and Charles B. Officer. The application of various geophysical techniques to specialized engineering projects. *Geophysics* 27:221-236. 1962.
8. Marine Geophysical Services Corporation. Continuous seismic profiler (sparker). Houston, Texas, 1961. 28 p.
9. Nafe, John E. and Charles L. Drake. Variation with depth in shallow and deep water marine sediments of porosity, density and the velocities of compressional and shear waves. *Geophysics* 22:523-552. 1957.
10. Oregon. Dept. of Geology and Geologic Investigation. Geologic map of Oregon west of the 121st meridian. Salem, 1961. (Miscellaneous Geological Investigation Map I-325)
11. Peters, L. V. The direct approach to magnetic interpretation and its practical applications. *Geophysics* 14:290-320. 1949.

12. Rinehart, W. A. and J. W. Berg, Jr. Nearshore marine gravity range, Newport, Oregon. Corvallis, 1963. 11 p. (Oregon State University, Department of Oceanography Data Report No. 9 on Office of Naval Research Contract Nonr 1286(02) Project NR 083-102 and National Science Foundation Grant No. G24353)
13. Snively, Parke D., Jr. and Holly C. Wagner. Tertiary geologic history of western Oregon and Washington. Olympia, 1963. 25 p. (Washington Division of Mines and Geology Report of Investigations No. 22).
14. Snively, Parke D., Jr. and Holly C. Wagner. Geologic sketch of northwestern Oregon. Washington, D. C., (in press). (U. S. Geological Survey Bulletin 1181).
15. Talwani, Manik, J. Lamar Worzel and Mark Landisman. Rapid gravity computations for two-dimensional bodies with application to the Mendocino submarine fracture zone. Journal of Geophysical Research 64:49-59. January, 1959.
16. Vacquier, V. et al. Interpretation of areomagnetic maps. Baltimore, Maryland, 1951. 151 p. (Geological Society of America Memoir No. 47).
17. Volkes, H. E., Hans Norbistrath and P. D. Snively, Jr. Geology of the Newport-Waldport area, Lincoln County, Oregon. Washington, D. C., 1949. 1 sheet. (U. S. Coast and Geodetic Survey Oil and Gas Preliminary Map 83).